Research Article

Modelling forest recolonization by an epiphytic lichen using a landscape genetic approach

Helene H. Wagner*, Silke Werth, Jesse M. Kalwij, Jacqueline C. Bolli and Christoph Scheidegger

*WSL Swiss Federal Research Institute, 8903 Birmensdorf, Switzerland; *Author for correspondence (e-mail: helene.wagner@wsl.ch)*

Abstract

The process of recolonization after disturbance is crucial for the persistence and dynamics of patch-tracking metapopulations. We developed a model to compare the spatial distribution and spatial genetic structure of the epiphytic lichen *Lobaria pulmonaria* within the perimeter of two reconstructed 19th century disturbances with a nearby reference area without stand-level disturbance. Population genetic data suggested that after stand-replacing disturbance, each plot was colonized by one or a few genotypes only, which subsequently spread clonally within a local neighborhood. The model (cellular automaton) aimed at testing the validity of this interpretation and at assessing the relative importance of local dispersal of clonal propagules vs. long-distance dispersal of clonal and/or sexual diaspores. A reasonable model fit was reached for the empirical data on host tree distribution, lichen distribution, and tree- and plot-level genotype diversity of the lichen in the reference area. Although model calibration suggested a predominance of local dispersal of clonal propagules, a substantial contribution of immigration of non-local genotypes by long-distance dispersal was needed to reach the observed levels of genotype diversity. The model could not fully explain the high degree of clonality after stand-replacing disturbance, suggesting that the dispersal process itself may not be stationary but depend on the ecological conditions related to disturbance.

Introduction

Landscape connectivity has been defined as the degree to which the landscape facilitates or impedes movement among resource patches (Taylor et al. 1993) or as the interaction between organism movement and landscape structure (Merriam 1984; Goodwin 2003). Hence, landscape connectivity has a structural component, i.e., the shape, size, and spatial arrangement of landscape elements, and a functional component, i.e., the re-

sponse of individuals to landscape features and the gene flow (by migration of animals or seed dispersal and pollen movement in plants) resulting from such response (Brooks 2003). While much of landscape ecological research deals with quantifying the structural component of connectivity, ecologists often aim at inferring from structural connectivity to functional connectivity. However, most of our understanding of how landscapes affect organism movement or the interactions among subpopulations stems from theoretical

work and computer simulation experiments (e.g., neutral landscape models; Gardner et al. 1987; With 1997), whereas empirical data testing the effect in real landscapes are relatively rare and may not be fully congruent with theoretical expectations (Harrison and Bruna 1999).

Functional connectivity is difficult to measure in terms of dispersal of individuals (Tischendorf and Fahrig 2000; Clobert et al. 2001). For sessile organisms such as plants, tracking the fate of individual propagules in the landscape is difficult and rarely done (Ouborg et al. 1999). The spatial distribution of organisms integrates many dispersal events, and habitat modelling may reveal whether a given species has been successful in colonizing most or all of its potential habitat (Ozinga et al. 2005). In addition, the spatial genetic structure of a population integrates gene flow including dispersal over a longer time span (Ouborg et al. 1999; Holderegger et al. in press), and genetic data allow, e.g., an estimation of the number of migrants exchanged per generation among populations (Beerli and Felsenstein 1999). With highly variable molecular markers such as microsatellites and under certain assumptions, the number of independent colonization events can be estimated for a haploid organism from the number of alleles at the most variable locus (Walser et al. 2003).

In plants, indirect estimates of gene flow based on the genetic structure of a population are often orders of magnitude lower than direct estimates based on propagule flow (Ouborg et al. 1999; Clobert et al. 2001), e.g., such as obtained by paternity analysis for gene flow by pollen (Sork and Smouse in press). One reason for this large discrepancy between direct and indirect estimates of gene flow is that population genetic data only reflect successful gene flow events (dependent on the sampling design). In organisms with clonal dispersal, the difference between the spatial patterns of clonality and of gene diversity may be used to discriminate between the dispersal processes of clonal and sexual propagules, e.g., pollen and seed in plants (Wagner et al. 2005; Werth et al. in press).

The effect of landscape structure on dispersal may be quantified by monitoring recolonization of disturbed areas in an experimental or quasi-experimental setting. However, such approaches are rare for several reasons. First, replication is difficult to accomplish at a landscape scale. Second, the relevant processes, e.g., patch dynamics and the generation time of the focal species, often lie beyond the time scale of ordinary research. Last but not least, such experiments may be resource-demanding or unethical to perform (Wiens et al. 1993; Peck 2004). Experimental model systems, such as percolation experiments of beetles in artificial model landscapes, represent a way of testing specific hypotheses on the effect of landscape pattern on biological processes (Wiens et al. 1993) and have shown the effect of landscape pattern on movement patterns of animals (With et al. 1999; Parker and Mac Nally 2002). However, extrapolation from experimental systems to functionally different types of organisms or landscapes is limited (Wiens et al. 1993).

Here, we propose to compare the spatial distribution and spatial genetic structure of an organism between landscapes differing in disturbance history, everything else being equal. However, true replicate landscapes with identical disturbance history are not available. In such situations, simulation modeling can be used to establish a mechanistic link between the spatial pattern of a landscape and the population dynamics of a focal organism. Hence, the observed data represent one possible outcome of population dynamics under disturbance, and modeling is used for inference about observed differences between local landscapes (Fortin et al. 2003) and for extrapolation to other landscapes and organisms.

We employed simulation modeling to compare connectivity of three nearby forested areas differing in stand history. We parameterized the model for the epiphytic, disturbance sensitive lichen *Lobaria pulmonaria*, a species predominantly growing on tree bark across a wide geographic range, covering both the temperate and boreal zone of the Northern and parts of the Southern Hemisphere (Yoshimura 1971). Although this lichen is both clonal and recombinant, it reproduces mainly clonally via soredia, isidia and to a lesser degree by thallus fragments (Scheidegger 1995; Walser et al. 2001; Denison 2003). Clonal propagules contain two of the three symbiotic partners, namely the mycobiont and its green algal photobiont (Jordan 1970). Hence, juvenile thalli originating from clonal propagation need to incorporate appropriate cyanobacteria strains, which have also been found in other lichens with

which *L. pulmonaria* is associated (Rikkinen et al. 2002). Young thalli originating from sexually produced ascospores need to find both green algal and cyanobacterial photobiontic partners in order to grow successfully. While clonal propagules of *L. pulmonaria* may be most suitable for within-site colonization, ascospores seem to be relevant for colonization of forests at large distances (Werth et al. in press). Highly variable microsatellites are available for the mycobiont (Walser et al. 2003). Molecular genetic data and diaspore dispersal estimates indicate that *L. pulmonaria* might rarely disperse over long distances of hundreds of meters (Walser et al. 2001; Walser 2004; Werth 2005). Dispersal limitation may explain why this lichen is often associated with forests with long ecological continuity or old-growth forests (Rose 1976, 1992). Within such habitats, however, it also grows on early-successional tree species (Snäll et al. 2005; Kalwij et al. in press).

Snäll et al. (2005) modeled the metapopulation dynamics of *L. pulmonaria* as a patch-tracking organism in a dynamic forest landscape model with natural and anthropogenic fire regimes. They found that the lichen is susceptible to fire suppression because of decreasing host tree regeneration in the absence of disturbance. On the other hand, lichen persistence under a forest fire disturbance regime critically depends on the ability of the lichen to recolonize disturbed stands. While Snäll et al. (2005) had extensive distributional data of the lichen and general information on the historical disturbance regime in their study region, they could not investigate the details of the recolonization process as they lacked both a spatially explicit reconstruction of individual disturbances and lichen genetic data that would allow to discriminate between the number of independent recolonization events and clonal spread within a disturbed area.

This study uses a modeling approach to compare the spatial distribution and spatial genetic structure of *L. pulmonaria* within the perimeter of two reconstructed 19th century disturbances with a nearby reference area that did not undergo any stand-level disturbance during the last 200 years. The disturbance types and the tree and lichen population dynamics are modeled in order to provide a mechanistic link between the reconstructed stand history and the observed distribution and genetic structure. The model should answer two specific questions: (1) whether the differences in the disturbance regime, everything else being equal, can explain the observed differences in the lichen population, and (2) how important long-distance dispersal (of clonal and/or sexual propagules) is in comparison to local dispersal of only clonal propagules.

Methods

Field data

Kalwij et al. (in press) performed a survey of potential and colonized host trees of *L. pulmonaria* in 251 circular plots of 1 ha sampled randomly from the wooded parts of the study area in the Parc Jurassien Vaudois, Switzerland (Figure 1). Potential host trees were defined as Sycamore maple (*Acer pseudoplatanus*) or beech (*Fagus silvatica*) with a diameter at breast height (dbh) exceeding 10 cm. Kalwij et al. (in press) reconstructed the perimeter of two 19th century stand-level disturbances reported in historical documents (Vittoz 1998) using aerial photographs from 1933. The 'burnt' area was heavily logged in 1870, followed by a wind throw and, in the following year, a 2-week fire. Tree-ring analysis (Bolli et al., WSL Birmensdorf, unpubl. data) of the oldest spruce trees on a 100-m grid suggested a stand-replacing disturbance in an area more or less consistent with the delineation in Kalwij et al. (in press), but with an island of surviving trees in the center of the disturbed area, including at least one remnant maple tree. The 'logged' area was subject to intensive logging for charcoal production over the second half of the 19th century, possibly with selective harvesting of spruce (*Picea abies*) and beech.

Werth et al. (in press) collected lichen samples from a subsample of colonized plots, selecting plots from within and around the 'burnt' and 'logged' areas and from a reference area without stand-level disturbance ('reference') that had a high density of both maple and the lichen (Figure 2). As all forests in the study area, the reference area was subject to uneven-aged forestry where individual trees of any age class are removed in order to maintain a heterogeneous stand structure (Schütz 2002). A maximum of 24 thalli was randomly selected from different trees in each plot.
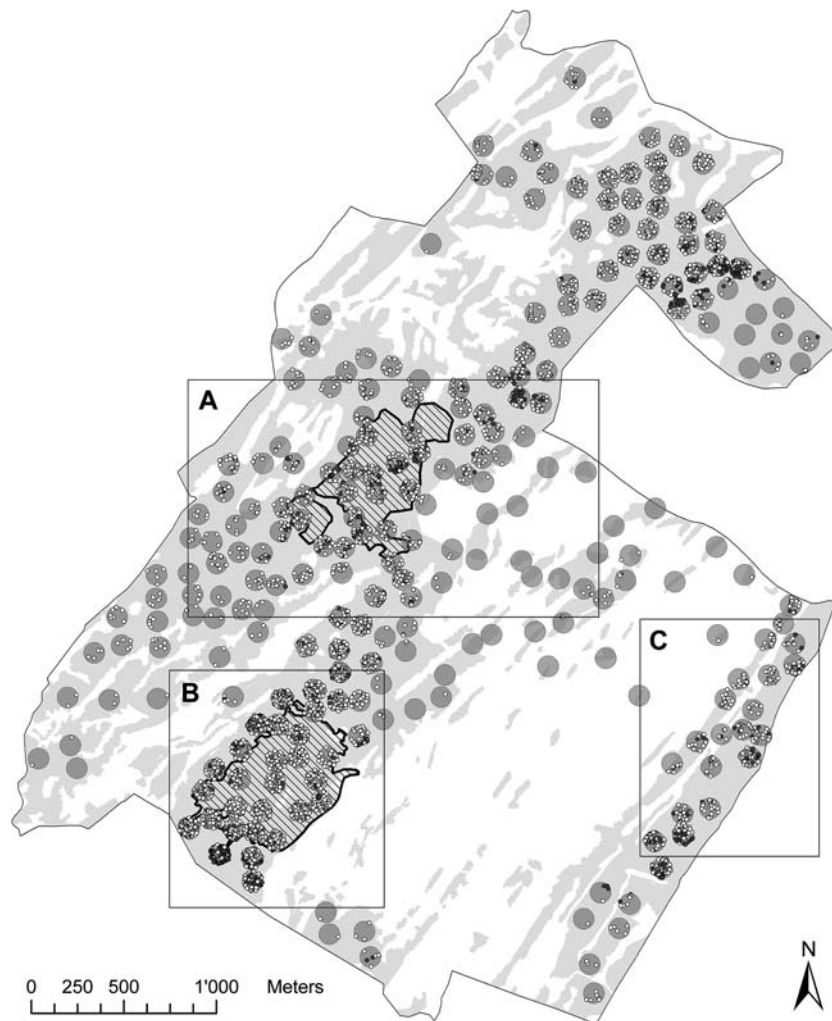
Figure 1. Map of all host trees colonized (black dots) and uncolonized (white dots) by *Lobaria pulmonaria* in a survey of 251 plots of 1 ha (grey circles) chosen randomly from the wooded part (light gray) of the study area in the Parc Jurassien Vaudois, Switzerland. Hatched polygons indicate the reconstructed perimeter of two 19th century disturbances based on aerial photo interpretation. Boxes A–C mark the extent of the detailed maps in Figure 2.
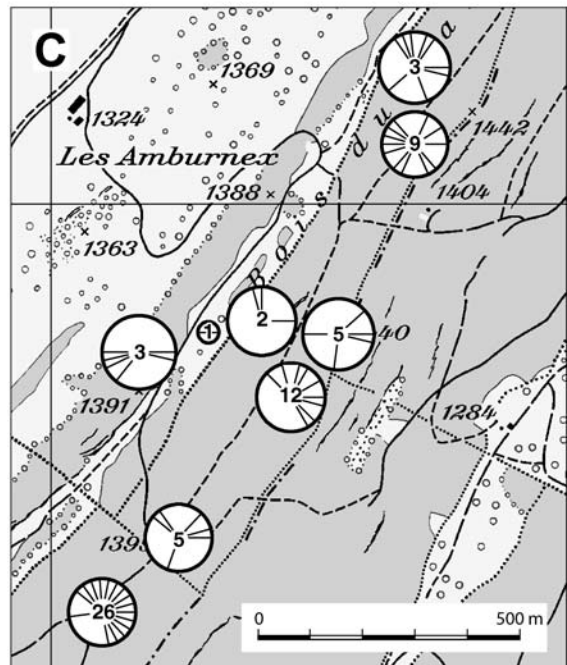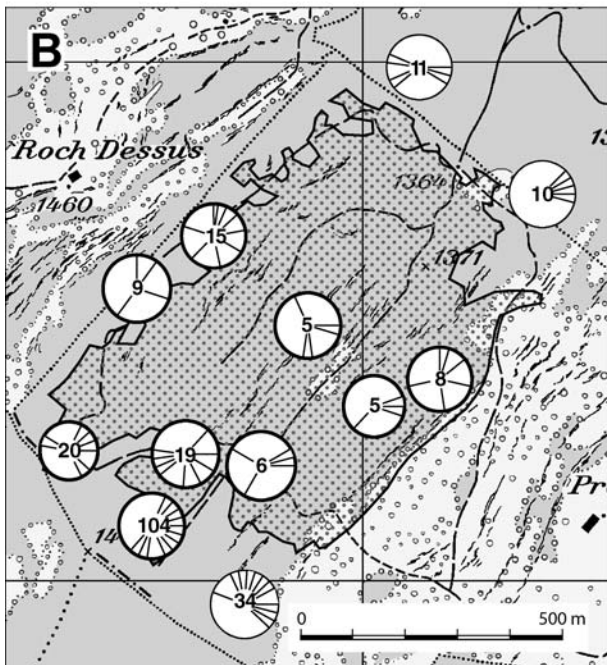
If there were fewer than 24 colonized trees, multiple thalli were sampled from the same tree, and if there were fewer than 24 thalli in a plot, every thallus found was included. The multilocus genotype of each sampled thallus was determined using six microsatellites specific to the haploid mycobiont (LPu03, LPu09, LPu15, LPu16, LPu20, LPu27). DNA extraction and fragment length determination using an ABI 3100-Avant automated sequencer (Applied Biosystems) followed Walser et al. (2004). Allele assignment was performed using GENOTYPER 2.5 (Applied Biosystems).

In the two disturbed areas, only a part of the plots fell within the reconstructed perimeter of the disturbances. Lichen reference data were restricted to those plots lying partially or entirely within the disturbance perimeter (Figure 2). Hence, the

Figure 2. Maps of genotype distribution in all 1-ha plots in the three subareas 'burnt' (A), 'logged' (B), and 'reference' (C). The number indicated in each circle shows the number of trees colonized by *Lobaria pulmonaria*, sectors reflect the relative frequency of genotypes, and circle size is proportional to the number of sampled thalli per plot. A bold outline indicates plots used as lichen reference data. Base map reproduced by permission of Swisstopo (BA057486).
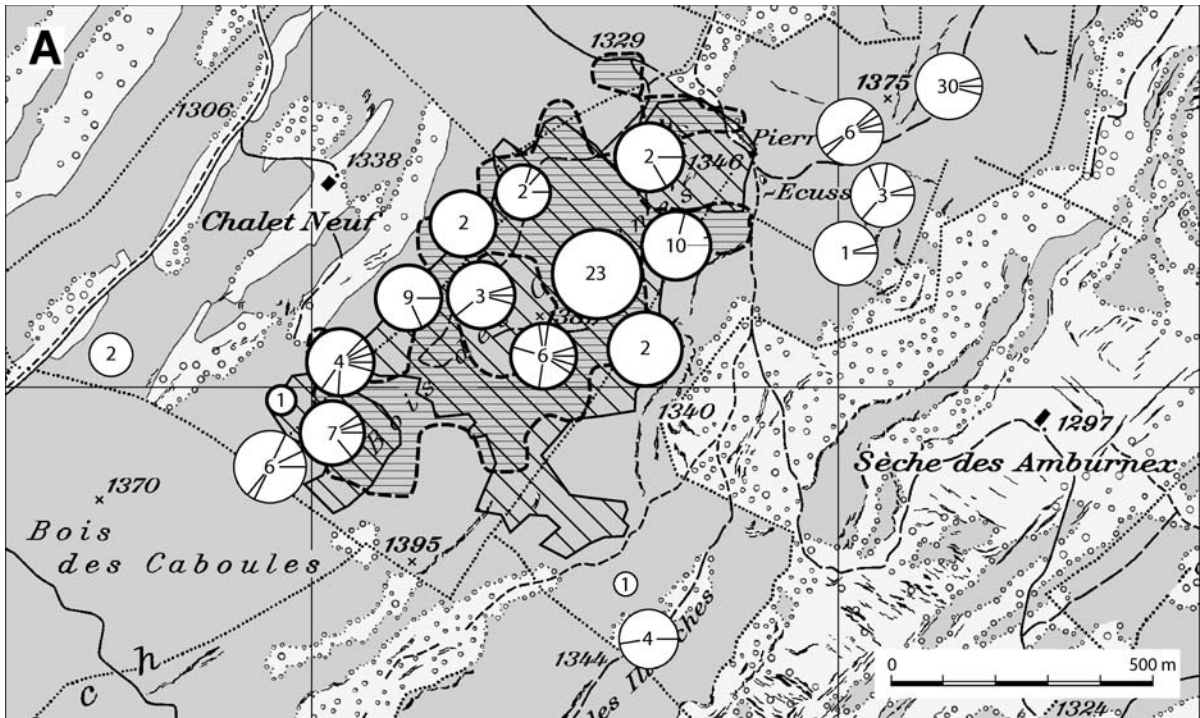
Disturbed area, affected by 1871 logging, windthrow, or fire; based on aerial photographs

Disturbed area, affected by 1871 logging, windthrow, or fire; based on tree-ring analysis

Disturbed area, affected by logging 1850-1900

Forest

Pasture

Stand-level disturbance	→	Tree dynamics	→	Lichen dynamics	→	Target variables

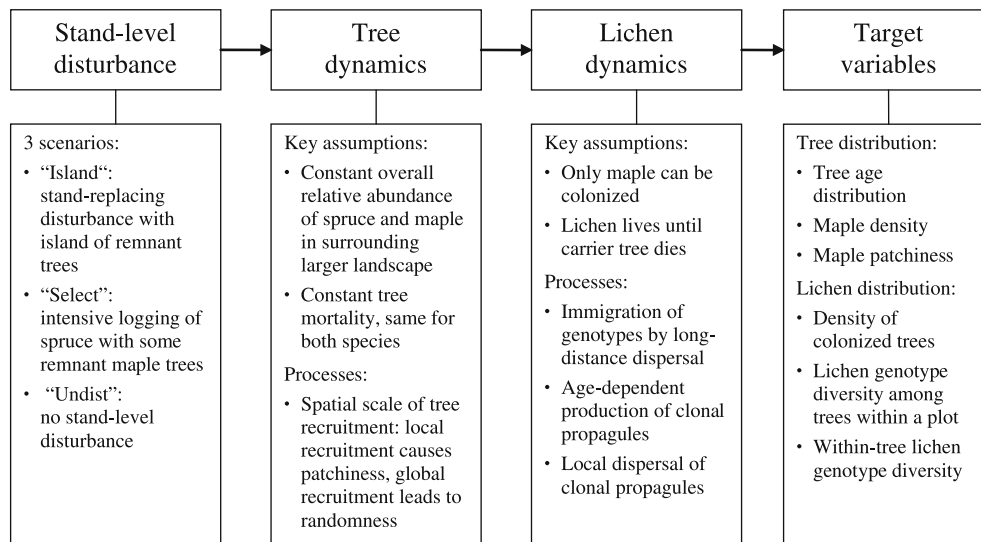| 3 scenarios: • "Island": stand-replacing disturbance with island of remnant trees • "Select": intensive logging of spruce with some remnant maple trees • "Undist": no stand-level disturbance	Key assumptions: • Constant overall relative abundance of spruce and maple in surrounding larger landscape • Constant tree mortality, same for both species Processes: • Spatial scale of tree recruitment: local recruitment causes patchiness, global recruitment leads to randomness	Key assumptions: • Only maple can be colonized • Lichen lives until carrier tree dies Processes: • Immigration of genotypes by long-distance dispersal • Age-dependent production of clonal propagules • Local dispersal of clonal propagules	Tree distribution: • Tree age distribution • Maple density • Maple patchiness Lichen distribution: • Density of colonized trees • Lichen genotype diversity among trees within a plot • Within-tree lichen genotype diversity

Figure 3. Overview of model structure with three scenarios, key assumptions and simulated processes of tree and lichen dynamics, and target output variables.

number of plots from the 'burnt', 'logged', and 'reference' subareas used for calibration was 21, 24, and 15 for tree data and 12, 9, and 9 for lichen genetic data.

Model structure and specification

The model simulates the dynamics of two tree species (maple and spruce) and the population dynamics of the lichen, separately for three subareas that differ in their stand-level disturbance history but are otherwise assumed identical (Figure 3). Each time step of 1 year begins with determining tree mortality, with lichen mortality directly linked to tree death. Dead trees are replaced, lichen propagule production is assessed, and (multiple) colonization of suitable trees is modeled as a function of local and long-distance dispersal. Technically, the model was implemented by linking a cellular automaton (CA) of tree dynamics with a CA of lichen dynamics, using Borland C++ Builder Version 6 (URL: http://www.borland.com). Three disturbance scenarios were specified, and the resulting patterns of tree distribution, lichen occurrence and lichen genotype diversity were exported and evaluated in R (Ihaka and Gentleman 1996).

Each CA consisted of 128×128 cells of an assumed size of 6.25 m $\times$ 6.25 m, so that the simulated area covered 8×8 ha. Each cell could only be occupied by a single tree, which amounts to 256 trees/ha. Analysis of LiDAR data suggested an average of 183.2 ± 9.6 trees per ha (Kalwij 2005), but this figure is probably too low, as small trees were likely to go undetected.

In order to keep the model simple, we made a number of assumptions: (i) the environment is spatially and temporally homogeneous except for disturbances; (ii) uneven-aged forestry leads to the same dynamics as natural dynamics (Schütz 2002); (iii) cattle grazing and ungulate browsing have no effect, or this effect is the same everywhere; (iv) no density-dependence of the lichen; (v) no selection, i.e., all lichen genotypes have the same fitness. Some further assumptions are discussed below.

Key parameters were calibrated by comparison of simulation results to target variables from field data, while other parameters were treated as fixed to reduce complexity (Table 1). The fixed parameters were varied in preliminary simulations, however, and their effect on the performance of the final calibrated model was assessed in sensitivity analysis. Parameter estimates for fixed parameters are explained in a separate section.

Table 1. Definition of fitted and fixed model parameters.

Parameter	Definition	Value	Unit
Tmean	Mean of exponential tree age distribution	Fitted	Years
pMaple	Global percentage of maple trees	Fitted	%
pRemnant	Percentage of maple trees retained in 'select' scenario	Fitted	%
pLocal	Percentage of trees recruited locally within 3×3 window	Fitted	%
maxSor	Maximum number of clonal propagules (soredia) produced	Fitted	Propagules/thallus/year
nLongd	Number of immigrating propagules (clonal or sexual) for entire simulated landscape	Fitted	Propagules/year
pInit	Initial mean number of thalli per tree	0.2	Thalli/tree
pEstab	Probability that a propagule arriving in a cell with a suitable host tree establishes	0.4	%
minAge	Minimum tree age for colonization	20	Years
genTime	Minimum thallus age for clonal reproduction	20	Years
mDist	Mean dispersal distance	40	Meters
isle	Logical flag determining whether an island of remnant trees should be simulated in the 'island' scenario	yes	Logical

Tree dynamics module

Beech, which contributed less than 2% of colonized trees (Kalwij 2005), was excluded from the model. The simplified model system contained two tree species, where maple is the lichen host tree and spruce cannot be colonized by the lichen. Both tree species were assumed to exhibit a negative exponential age distribution with a mean of *Tmean*, which was simulated using a constant mortality function with a yearly probability of death of $1/Tmean$.

Differences in lichen distribution due to a successional increase of maple after stand-replacing disturbance were ruled out by the selection of a reference area 'reference' with the same maple density as the 'burnt' area. Hence, in our model, the two tree species differed only in total abundance (defined as the relative abundance of maple, *pMaple*) and in their suitability as lichen habitat. The significantly higher maple density in the 'logged' area was attributed to selective logging for spruce, effectively retaining some proportion *pRemnant* of the maple population.

The main factor in our tree dynamics model was the spatial scale of tree recruitment, i.e., the rule by which an adult tree was immediately replaced by another mature tree (no cohort structure). Two extreme cases are possible. First, seed dispersal is not limited, so that any seed can get anywhere and the species of a new tree is sampled according to the overall relative abundance as defined by *pMaple* (global recruitment). This parameter was kept constant during each simulation because it reflects the average proportion of trees in a larger surrounding area not affected by the simulated disturbance. Second, seeds disperse only to the neighboring grid cell, so that the species of a new tree is sampled from a neighbourhood of 3×3 cells, including the dead tree (local recruitment). Intermediate scenarios were derived by defining the probability *pLocal* with which a seed was locally recruited.

Lichen dynamics module

Lichen population dynamics was defined by immigration rate, local reproduction rate and dispersal function of clonal propagules, establishment rate, and mortality due to tree death. Population dynamics was modelled for each genotype independently, but with identical parameters. We did not explicitly model recombination, as we rarely observed apothecia in the field and preliminary simulations suggested that even high levels of recombination improved model fit only slightly. However, recombination was incorporated implicitly as immigration of new genotypes.

We assumed that once a propagule arrives in a cell with a suitable tree, it successfully establishes with probability *pEstab*. All maple trees older than *minAge* were considered suitable for colonization (see below). We did not vary *pEstab* as a function of tree age because we found an extremely weak correlation between tree age and dbh for maple trees from a stand within the study area (Stähli et al., WSL Birmensdorf, unpubl. data).

The production of clonal propagules (soredia) was assumed to increase logistically starting from a minimum age for clonal reproduction *genTime* (see below), eventually reaching a constant maximum level of *maxSor*. The number of soredia produced by a thallus in a given year was thus derived as $N = \text{trunc} (0.5 + maxSor * \exp(z)/(1 - \exp(z)))$, where ($z = -11.5 * 0.35 * Thallus\text{-}Age$). Local dispersal of soredia was simulated by sampling a distance $d \sim g(d) = \text{e}^{-ad} * 0.05^2 * d$ (see below) and a direction $\phi = [0, 2\pi]$ for each propagule. A scaling factor allowed manipulating the mean dispersal distance *mDist*.

The probability p that a suitable maple tree was colonized by long-distance dispersal was modelled as a function of a constant number *nLongd* of immigrating propagules of all genotypes, with $p = 1 - (1 - pEstab * 1/128^2)^{nLongd}$. We chose a constant immigration rate p to each cell because disturbance was assumed to reduce population size locally but not in the surrounding larger landscape. The colonizing genotype was sampled randomly based on the observed allele frequencies in all sampled thalli.

Estimates of fixed parameters

pEstab: We assumed that the total probability that a propagule arriving in a cell with a suitable maple tree will hit a suitable substrate on the bark of the tree and successfully establishes at *pEstab* = 0.004. This parameter is essentially a scaling factor that affects the absolute values of *maxSor* and *nLongd*, but not their ratio, i.e., the relative importance of the two dispersal processes does not depend on the value of *pEstab*.

minAge: Although young maple trees are rarely colonized by *L. pulmonaria* due to their smooth bark, the empirical definition of a minimum age for colonization is difficult. Our primary concern was to avoid overestimation of this minimum age, which might cause artificially high differences in lichen abundance between undisturbed and disturbed plots, especially as trees would be expected to grow fast due to increased light after stand-level disturbance. Hence we assumed a conservative value of *minAge* = 20 years, which is deliberately lower than the 30 years suggested by Scheidegger et al. (1998) for an undisturbed stand from the northern Alps.

genTime: Although some early production of soredia has been reported from a 14 year old thallus (Scheidegger et al. 1998), significant propagule production is not expected before age 35 (Scheidegger and Goward 2002). We assumed a logistic relationship between soredia production and thallus age centred at 35 years. After age 20, soredia production thus increased logistically up to age 50 and continued at a constant maximum level (*maxSor*) until the death of the host tree.

mDist: Werth (2005) estimated local dispersal of soredia from molecular analysis of *L. pulmonaria* DNA in snow samples taken at various distances up to 40 m from a source tree and from tree-level occurrence data. Averaged over all directions, both approaches suggested an exponential distribution $f(d) = a\text{e}^{-ad}$ of propagule density at distance d from a source, with rate $a = 0.05$ (Werth 2005). In two-dimensional space, the corresponding isotropic density of dispersal distance for the propagules is $g(d) = f(d) * a * d$, where the multiplication by a ensures that the total area under the curve equals 1 (Werth 2005). The mean dispersal distance $mDist = 2/a$ was estimated at 40 m.

Disturbance module

We simulated two types of deterministic disturbance mimicking our conception of the two historical disturbances. In analogy to the 'burnt' area, all trees from the central 6×6 blocks of 1 ha were eliminated, with the exception of the trees from a central island of 2×2 blocks ('island' scenario). A logical flag *isle* allowed the omission of this island for sensitivity analysis. As an analogue to the 'logged' area, trees from the entire central 6×6 blocks of 1 ha were removed, but a certain percentage (*pRemnant*) of randomly selected maple trees was retained ('select' scenario).

Replicate simulations

Each replicate simulation started with initialization of the tree grid and a spin-up run of 200 years to allow the spatial tree pattern to develop. The tree grid was initialized randomly according to the overall proportion of the two species defined by *pMaple*. Initial tree age was sampled from a uniform distribution between [1, 200], which had no influence on simulation results as the spin-up run was long enough to reach the targeted exponential tree age distribution with mean *Tmean*. To initialize the lichen grid, the number of initially present lichen thalli was determined for each suitable tree (maple ≥ 20 year) from a Poisson

process with a mean of *pInit* = 0.2. This value corresponds to the proportion of colonized host trees estimated from the reference subpopulation. Initial thallus age was sampled from a uniform distribution between 1 and the age of the host tree minus 20. The multilocus genotypes were determined in the same way as for immigration by long-distance dispersal. We assumed periodic boundary conditions to allow the local immigration of genotypes.

After another spin-up run of 200 years, both grids were saved as a common starting point for simulation under the three disturbance scenarios. At this time, a disturbance option was run once for each scenario (either 'island', 'select', or none for the undisturbed scenario 'undist') and the simulation continued for another 130 years, after which the final simulation results were evaluated. Simulation parameters and two lists were exported, one containing all trees with their location, species, age, and number of thalli and genotypes, another listing all lichen thalli with their location, age, and genotype. Simulations were stopped if a total population size of 50,000 thalli was exceeded.

Evaluation of simulation results
For model evaluation, a 16-cells wide edge was excluded in order to limit the extent to the area subjected to disturbance and to avoid edge effects. Thalli were subsampled within each plot of 1 ha (16×16 cells) mimicking the sampling by Werth et al. (in press). The target variables evaluated for

each scenario in each replicate simulation and for the reference data are defined in Table 2.

The six target variables were combined hierarchically into a model performance index (MPI; Villa et al. 2004). The basic criteria (indicated by the prefix 'c_') were defined by the minimum of the ratio of the simulated value to the reference value and their inverse ratio. Hence, each criterion was scaled to increase linearly from a simulated value of zero to a simulated value equal to the reference value, and then decay towards zero as the simulated value approaches infinity. This definition ensured that each criterion varied over the entire parameter space while approximating symmetric behavior near the maximum. The scores were calculated for each scenario and weighted equally in the calculation of the overall score for each criterion. A first index was derived to assess goodness of fit to the tree data (MPIT):

$$MPIT = 0.33 * c\_nMaple + 0.33 * c\_mAge + 0.33 * c\_sdMaple.$$

The total MPI was defined as:

$$MPI = 0.25 * MPIT + 0.25 * c\_nCol + 0.25 * c\_pDiv + 0.25 * c\_tDiv,$$

thus giving equal weight to the four components of tree distribution, lichen occurrence, plot-level and tree-level lichen genetic diversity.

There was high variance among replicate MPI values, and the response surface was complex, especially in the case of lichen genetic diversity

Table 2. Definition of target values derived from simulation output and reference data.

Parameter	Simulation output	Reference value if different	Unit
nMaple	Mean number of maple trees of at least minAge years per plot	Mean number of maple trees with dbh >10 cm per plot	Trees/plot
mAge	Median age of the oldest tree (spruce or maple) within a 8×8 cells from center of each block of 16×16 cells (scenario 'undist' only)	Median age of spruce trees sampled by Bolli et al. (WSL Birmensdorf, unpubl. data) from outside disturbance perimeter	Years
sdMaple	Standard deviation of the number of maple trees per plot		Trees/plot
nCol	Mean number of colonized trees per plot		Trees/plot
pDiv	Average within-plot genetic diversity of the lichen, defined as the probability that two thalli sampled from two different trees have different genotypes.		%
tDiv	Average within-tree genetic diversity of the lichen per plot, defined as the probability that two thalli sampled from the same tree have different genotypes, averaged over all sampled trees within a plot and subsequently over all plots.		%

Table 3. Calibration of tree dynamics.

Step	nSim	nRep	Level	Tmean		pMaple		pLocal		pRemnant	
				lower	upper	lower	upper	lower	upper	lower	upper
1	200	3	–	30	100	0.05	0.25	0.00	1.00	0.00	1.00
2	100	3	0.80			0.12	0.18	0.85	1.00	0.20	0.70
3	1000	3	0.85			0.12	0.18	0.95	1.00	0.20	0.50
4	50	3	0.94			0.15	0.16	0.97	0.99	0.35	0.45
Final				54		0.155		0.98		0.39	

The table lists for each calibration step the number of selected parameter combinations (*nSim*), the number of replicate simulations per parameter combination (*nRep*), and the threshold level of MPIT (*Level*) used to determine the lower and upper bounds of values for the expected mean tree age (*Tmean*), the expected proportion of maple (*pMaple*), the probability of local tree recruitment (*pLocal*), and the proportion of maple retained in the 'select' scenario (*pRemnant*). The last line contains the fitted parameter estimates.

defined by the combination of *c_pDiv* and *c_tDiv*. Due to constraints on computation time, it was not feasible to base calibration solely on an optimization of MPI values either by Monte Carlo techniques or by numerical optimization algorithms such as a gradient approach, simulated annealing, or a genetic algorithm. Assuming the response surface of MPI to be smooth without sudden narrow peaks, we opted to simplify the problem by two means. On one hand, we fitted parameters sequentially in three groups: first *Tmean*, which showed little interaction with the other parameters, then the other parameters of tree dynamics, *pAcer*, *pLocal* and *pRemnant*, and finally the parameters of lichen dynamics, *nLongd*

Table 4. Calibration of lichen dynamics.

Step	nSim	nRep	Level	nLongd		maxSor	
				lower	upper	lower	upper
1	100	3		0	0	10	200
2	100	3		1000	30000	0	0
3	100	3		0	15000	0	100
4	50	3	0.70	1500	9000	30	100
5	75	30	0.72	3000	7500	50	90
6	50	30	0.725	4500	6000	60	80
Final				5000		72	

The table lists for each calibration step the number of selected parameter combinations (*nSim*), the number of replicate simulations per parameter combination (*nRep*), and the threshold level of MPI (*Level*) used to determine the lower and upper bounds of values for the total number of immigrating propagules per year (*nLongd*) and the maximum yearly soredia production per thallus (*maxSor*). The last line contains the fitted parameter estimates.

and *maxSor*. On the other hand, we used MPI to reduce the multivariate parameter space using several sets of Monte Carlo simulations, reducing parameter range sequentially after each set (Table 3). The parameter values were then fitted from scatter plots of individual simulated MPI values against each parameter or from a response surface defined by a pair of parameters.

To fit the four parameters of tree dynamics, 200 parameter combinations were sampled from an initial, large range of *Tmean*, *pMaple*, *pLocal*, and *pRemnant* as defined in Table 3, where each range was divided equidistantly into 32 values. Three replicate simulation runs were carried out with each parameter combination, and model evaluation was based on the median of the three replicate simulation results. While three simulations are not enough for a reliable point estimate, we considered it sufficient for a first identification and exclusion of a range of highly unlikely parameter values. In order to fit *Tmean*, the simulated median age *mAge* (see Table 2 for definition) was regressed against *Tmean* ($R^2 = 0.99$, *p*-value < 0.001). The reference value of *mAge* = 233 years corresponded to a *Tmean* of 54.

A restricted range of parameter values was derived from the settings of simulations that resulted in a MPIT > 0.80. The simulation and range reduction process was repeated three times with varying number of parameter combinations, replicate simulations, and MPIT levels as summarized in Table 3. For each of the three remaining factors, a loess regression model was fitted for the 50 parameter combinations from the last step, and the parameter was estimated visually from the maximum of the fitted curve.

Table 5. Sensitivity analysis: Effect of a 20% change in each fitted or fixed parameter while keeping all others constant.

Type	Parameter varied	fitted value	new value	c_nMaple	c_mAge	c_sdMaple	c_nCol	c_pDiv	c_tDiv	MPI
Fitted model	none			0.94	0.98	0.76	0.71	0.81	0.50	0.73
Fitted parameters	*Tmean*	54	44	0.91	**0.80**	0.75	**0.59**	0.81	0.49	**0.68**
			64	0.93	**0.85**	0.78	**0.60**	*0.83*	0.46	**0.69**
	pMaple	0.155	0.125	**0.83**	0.98	0.79	**0.60**	0.81	0.52	**0.70**
			0.185	**0.86**	0.98	0.77	0.67	*0.82*	0.48	0.71
	pLocal	0.98	0.80	**0.80**	0.98	**0.44**	0.64	0.80	*0.54*	**0.68**
			1.00	**0.78**	0.98	**0.65**	0.64	0.81	*0.48*	**0.68**
	pRemnant	0.39	0.31	0.94	0.98	0.78	0.72	0.81	0.53	0.74
			0.47	0.95	0.99	0.79	0.67	0.81	0.51	0.73
	maxSor	72	58	0.94	0.98	0.77	0.64	0.81	0.49	0.71
			86	0.95	0.98	0.78	0.66	0.80	0.52	0.72
	nLongd	5000	4000	0.93	0.97	0.77	0.67	0.80	*0.54*	0.73
			6000	0.94	0.98	0.77	0.67	0.82	*0.48*	0.72
Fixed parameters	*isle*	yes	no	0.93	0.98	0.75	0.67	0.81	0.50	0.72
	pInit	0.2	0.16	0.93	0.98	0.75	0.67	0.81	0.50	0.72
			0.24	0.94	0.98	0.78	0.69	0.81	0.52	0.72
	pEstab	0.04	0.032	0.94	0.98	0.78	**0.62**	0.80	*0.55*	0.72
			0.048	0.94	0.97	0.78	**0.62**	0.81	*0.53*	0.71
	minAgeCol	20	16	0.94	0.97	0.77	0.68	0.82	0.50	0.72
			24	0.94	0.97	0.79	0.69	0.81	0.52	0.73
	genTime	20	16	0.95	0.98	0.80	0.67	0.81	0.52	0.73
			24	0.94	0.99	0.79	0.68	0.81	0.52	0.73
	mDist	40	32	0.95	0.98	0.79	0.70	*0.79*	*0.54*	0.73
			48	0.95	0.97	0.77	0.70	0.82	0.49	0.72

The table lists for every target variable and for the total MPI the median value obtained from 20 simulations. Bold numbers indicate values significantly different from those of the fitted model (Wilcoxon test, Bonferroni correction, $\alpha = 0.05/161$). Values for genotype diversity *pDiv* and *tDiv* significant at a less restrictive level of 0.05 are in italics. The values for the fitted model are provided as reference. See text for definitions of parameters and target criteria.

For fitting the lichen dispersal parameters *nLongd* and *maxSor*, we adapted the above procedure to account for the strong interaction between the two parameters (Table 4). In order to determine the range of possible models, we first searched for the best fitting model involving long-distance dispersal only, then the best model with local dispersal of propagules only. Based on these upper bounds for *nLongd* and *maxSor*, we further restricted the range of parameter values by fitting a trend surface to MPI as a function of the two parameters, using the function ordisurf from the R library vegan. As MPI was bounded by [0,1], we used a quasibinomial GAM model with 10 knots. In each step, the range of parameter combinations resulting in an average MPI higher than a given threshold level was determined visually from a contour plot of the trend surface. Note that *pEstab*, *nLongd* and *maxSor* are linked: increasing *pEstab* and decreasing both *nLongd* and *maxSor* (keeping their ratio constant) by the same factor has no effect on simulation results.

Sensitivity analysis

All fixed parameters (*pEstab*, *pInit*, *minAge*, *genTime*, *mDist*, *isle*) were subjected to sensitivity analysis, varying one parameter at a time. For reasons of comparability, the procedure was repeated for all fitted parameters (*Tmean*, *pLocal*, *pMaple*, *pRemnant*, *maxSor*, *nLongd*). For each parameter, the median MPI and the median of each of the six criteria contributing to MPI were determined from 20 replicate simulations for each of two new parameter values corresponding to 0.8 and 1.2 times the fitted value (Table 5). We found this level of replication sufficient for a robust estimate of the order of magnitude of each effect. The medians of the two lichen diversity criteria *c_pDiv* and *c_tdiv* were calculated twice, once averaged over all three scenarios (as in calculating MPI) and once based on scenario 'undist' only. For each criterion and each parameter value, the significance of the difference from the values obtained for the fitted model was assessed by a Wilcoxon test. To account for the large number of tests, a Bonferroni correction was applied, dividing
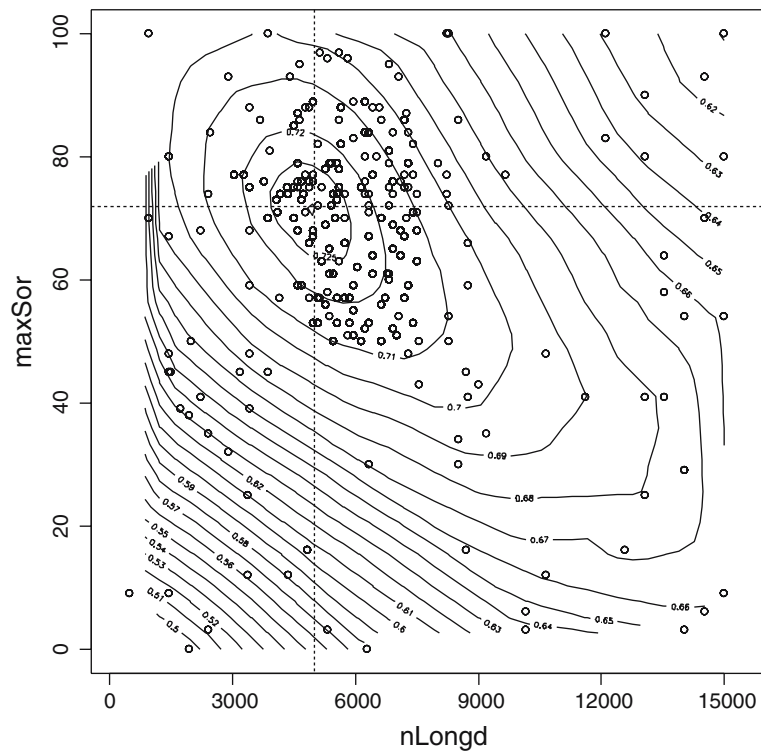
Figure 4. Fitted trend surface of MPI as a function of clonal reproduction rate *maxSor* and (clonal or recombinant) propagule immigration rate *nLongd*. Each point denotes a parameter combination with 3–30 replicate simulations (Table 4). The broken lines indicate the fitted parameters of the final model.

the significance level of 0.05 by the number of tests.

Results

Model calibration

Calibration of the tree dynamics model resulted in 98% local tree recruitment (*pLocal*), suggesting a surprisingly strong patchiness (Table 3). Almost 40% of maple trees needed to be retained (*pRemnant*) in order to reach a maple density *nMaple* in the 'select' scenario that matched the density observed in the 'logged' area. Fitting *pRemnant* to the lichen distribution data, however, resulted in a reduction of the retention rate to 20% (calibration results not shown).

The range of possible models was delimited by the models fitted to long-distance dispersal only, with *nLongd* estimated at 15,000, and to local dispersal of clonal propagules only, with *maxSor* estimated at 100 (Table 4). The best fitting model

combining the two processes contained 72% of this maximum value for *maxSor*, but only 33% for *nLongd*. The fitted response surface (Figure 4) indicated that relatively good fits may be obtained for high values of *maxSor* (50–90%) and lower values of *nLongd* (25–45%), thus delineating the range of realistic models.

The distributions produced by the fitted model approximated the observed distribution of trees (*nMaple*, *mAge*, *sdMaple*) and of lichens (*nCol*) quite well (Figure 5). Lichen genotype diversity *pDiv* and *tDiv* was better predicted for the reference area, whereas there were marked discrepancies especially for the 'island' scenario aimed at explaining patterns observed in the 'burnt' area.

Sensitivity analysis suggested that none of the fixed parameters had a strong effect on simulation results (Table 5). The only exception was establishment rate *pEstab* affecting the number of colonized trees *nCol*. Most of the fitted parameters of tree dynamics had a strong effect on tree patterns, where tree age distribution *mAge* naturally was
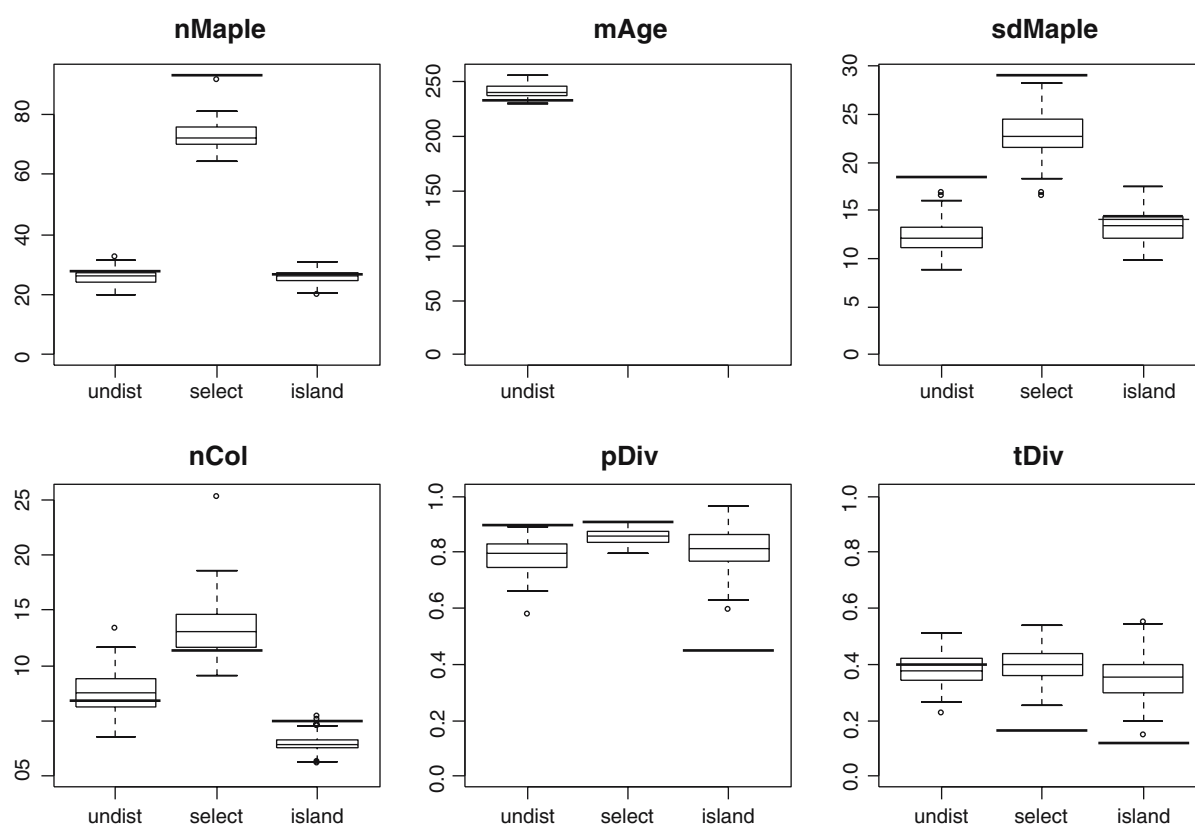
Figure 5. Comparison of the distribution of target variables produced by the fitted model with observed values. Each boxplot shows the distribution of a variable (Table 2) under a given disturbance scenario obtained from 100 replicate simulations of the fitted model as defined in Table 5, setting *pRemnant* to 20%. Bold lines indicate the reference values estimated from the field data.

affected by the tree mortality parameter *Tmean*, tree patchiness *sdMaple* depended on the spatial scale of tree recruitment *pLocal*, and the number of host trees *nMaple* responded to the overall relative abundance *pMaple* and *pLocal*. Surprisingly, the parameters for local (*maxSor*) and long-distance dispersal of soredia (*nLongd*) showed no significant effect on lichen genetic diversity *pDiv* and *tDiv* or on overall MPI. In fact, none of the parameters showed a statistically significant effect on lichen genotype diversity (*pDiv*, *tDiv*) in the sensitivity analysis when a Bonferroni correction was applied. The same result was obtained when using only the 'undist' scenario for assessing the effect of individual parameters on *pDiv* and *tDiv* (results not shown), suggesting that the robustness of the model was not due to a fitting trade-off. Rather, variability in these criteria was so high between replicate simulations that it prevented

these effects from becoming statistically significant (Figure 5).

When considering a less restrictive significance level of 0.05 for each test, most parameters of tree dynamics showed an effect on lichen genotype diversity (Table 5). The strongest relationships were between tree-level lichen genotype diversity *tDiv* and tree patchiness *pLocal*, lichen immigration rate *nLongd* and dispersal distance *mDist*. Plot-level lichen genotype diversity *pDiv* was affected by tree age distribution *Tmean*, host tree abundance *pMaple*, and dispersal distance *mDist*. Overall, the model was robust towards changes in the initial lichen density (*pInit*), assumptions regarding the minimum tree age for colonization (*minAge*) and minimum lichen age for clonal reproduction (*genTime*), and the presence of an island of remnant trees in the center of the disturbed area (*isle*).

Discussion

The field data on the spatial distribution and spatial genetic structure of the epiphytic lichen *L. pulmonaria* showed that the lichen had successfully recolonized both disturbed areas (Kalwij et al. in press). However, genotype diversity was considerably reduced within plots subjected to stand-replacing disturbance 130 years ago, suggesting the prevalence of local dispersal of clonal propagules after few independent colonization events per plot (Werth et al. in press). The model presented here aimed at assessing the validity of such an interpretation. Alternative explanations include stochasticity of the observed patterns, the confounding effect of other ecological factors and processes, or spatial heterogeneity of the dispersal process.

The field study was replicated at the plot level, but strictly speaking, each subarea represented a single outcome of the recolonization process (Fortin et al. 2003). The very high variance of simulation results suggests that replicate outcomes of a stand-level disturbance-recolonization experiment may vary considerably, even if all other factors are kept constant as in our simulation experiments. Specifically, there was a high variance of genetic diversity, which here referred to the diversity of haploid multilocus genotypes in the lichen mycobiont. Further research is needed to investigate whether such high variance among replicate processes is a common problem for landscape genetic studies.

Landscape dynamics may be expected to affect lichen genetic diversity negatively. This is because disturbance reduces patch persistence time, thus increasing the extinction probability of local populations (Keymer et al. 2000), and local extinctions may lead to decreased genetic diversity of the metapopulation (Ray 2001). In our simulations, lichen genetic diversity was indeed affected by several parameters related to landscape dynamics and configuration, namely tree patchiness *pLocal*, tree age distribution *Tmean*, and host tree abundance *pMaple*, especially at the tree level. Stochasticity in these habitat characteristics is likely to propagate and inflate variance in genetic data in addition to the stochasticity of lichen population dynamics. The latter may even be underestimated in our study as we did not explicitly model sexual reproduction, which is another source of variation. This illustrates that the results of landscape genetic studies of the effect of landscape structure and especially landscape dynamics on population genetic structure need to be interpreted with caution, unless there is sufficient replication at the landscape level, which will often be impossible to obtain.

Are observed differences due to disturbance alone?

In vascular epiphytes, lower genetic diversity was found for disturbed and spatially isolated populations than for undisturbed populations (Gonzalez-Astorga et al. 2004; Trapnell and Hamrick 2005). In our study, however, the observed differences in epiphytic lichen genetic diversity could not be fully explained by the hypothesized model. Parameter combinations that provided a reasonable fit with the number of colonized trees and with genotype diversity of the reference area could not explain the difference in genotype diversity between the reference and the two disturbed areas. As a result, it was not possible to determine a single best fitting model with a distinctly better fit than any other parameter combination, but a range of most realistic models was identified.

Spatial analysis previously showed that the size of clonal patches was considerably larger in the area of the stand-replacing disturbance than in the other two areas (Werth et al. in press). This was reflected also in a higher number of genotypes shared between plots. These findings suggest that the failure of the model to explain clonal patterns after the stand-replacing disturbance, while providing a good fit for the reference area, may not necessarily be due to problems of parameter estimation or the omission of important factors, but may result from a spatial heterogeneity in lichen population dynamics, i.e., gene flow may be complex and inhomogeneous across the population (Richards et al. 1999). Local site conditions for the survival of clonal propagules may have been particularly favorable in the area affected by stand-replacing disturbance. Competition is an important process hindering establishment of lichen propagules (Bailey 1976; Antoine and McCune 2004). Trees were virtually absent from the area affected by stand-replacing disturbance except for a group of trees in its center (Bolli et al., WSL Birmensdorf, unpubl. data). Major lichen and bryophyte competitors hindering propagule development of *L. pulmonaria* may have been

lacking on many of the regrowing trees. Alternatively, additional vectors such as birds or insects may have been available (Bailey and James 1979), changes in forest structure may have affected wind speed and turbulence and thus increased the likelihood of successful wind dispersal (Tackenberg 2003), soredia production may have been increased or generation time reduced due to favorable conditions. The latter may be explained by the larger growth rates in *L. pulmonaria* observed under forest edge conditions than in the forest interior (Sundberg et al. 1997), which may lead to a larger soredia production and faster completion of the life cycle on sites affected by stand-replacing disturbance.

How important is long-distance dispersal?

Even though an exact parameter estimate was not possible, the response surface defined by *maxSor* and *nLongd* suggested that local dispersal of clonal propagules is likely the dominant dispersal process (50–90% of the estimated maximum), but that a significant amount of long-distance dispersal (25–45% of the estimated maximum) is needed to explain the observed patterns. The importance of long-distance dispersal in structuring the spatial distribution of plant species and for metapopulation dynamics has been emphasized recently (Cain et al. 2000; Tackenberg 2003). Fertile thalli of *L. pulmonaria* develop apothecia for sexual ascospore production throughout the year (Denison 2003). The smaller and lighter ascospores may contribute considerably to long-distance dispersal (Bailey 1976), while the larger and heavier vegetative propagules may operate at short distances. This scenario would explain the small number of genotypes shared between plots and the high level of clonality within trees and among trees within plots (Werth et al. in press). However, long-distance dispersal is not necessarily correlated with weight or size of propagules (Cain et al. 2000). Differences in the number of fertile thalli may also be responsible for some of the difference in genetic structure among disturbance types. The recombination process in *L. pulmonaria* is still little understood, and the same is true for ascospore dispersal characteristics and establishment conditions (Walser et al. 2004). More research is needed to clarify under which conditions sexual reproduction occurs in *L. pulmonaria* and whether sexual propagules are mainly responsible for long-distance dispersal in this lichen.

Alternatively, what we modeled as long-distance dispersal may correspond to the tail of the dispersal distribution of clonal propagules, as our definition of immigration of new genotypes by long-distance dispersal did not discriminate between clonal and sexual reproduction. Different dispersal kernels differ in their shape and especially in their tails, and a fat tail distribution may have important effects on the spread of a population, colonization of habitat patches, and the persistence of a metapopulation (Clark 1998). The lognormal model used by Snäll et al. (2005) for modeling metapopulation dynamics of *L. pulmonaria* has a fatter tail than the exponential model. Over the 40–50 m investigated by Werth (2005), however, the exponential model fitted both the snow sample and the occurrence data from our study area much better than the lognormal model. More importantly, we considered a lognormal model of propagule density inappropriate for theoretical reasons. In two-dimensional space, it predicts a steady increase in the probability density function of dispersal distances with distance from the source. This problem is related to the asymptotically infinite velocity of expansion of dispersal kernels with fatter tails than the exponential distribution (Kot et al. 1996), which implies that a fatter tail than the exponential model of propagule density is physically impossible. However, direction-dependent, anisotropic dispersal, turbulence, or the presence of additional vectors (see above) could increase the probability of long-distance dispersal events.

Conclusions

This study illustrates the use of a combination of modeling and molecular methods for quantifying functional connectivity so as to test the effect of landscape structure and disturbance. Specifically, we relied on genetic data for a direct quantification of clonal dispersal and for distinguishing between alternative colonization processes.

Population genetic data suggested that after stand-replacing disturbance, each plot was colonized by one or a few genotypes only, which subsequently

spread clonally within a local neighbourhood. However, the model could not explain this high degree of clonality, and complementary spatial analysis supported that gene flow may be inhomogeneous across the study area. If the dispersal process may not be assumed stationary in space and time, this poses a challenge to model parameterisation and limits comparability between studies (Lertzman and Fall 1998; Fortin et al. 2003; Wagner and Fortin 2005).

Functional connectivity depends on characteristics of the landscape and of the organism, and it is highly scale-dependent both in space and time. Here, landscape structure and dynamics were defined by the host tree density, spatial aggregation, and patch persistence in terms of tree mortality. The simulations showed that the number of colonized trees was affected by the overall density of host trees and their mortality. Lichen generation time had a far smaller effect than tree mortality rate, suggesting that the temporal scale of connectivity was determined by the host tree dynamics. The spatial aggregation of host trees mainly influenced lichen genotype diversity at the tree level, whereas the mean lichen dispersal distance affected both tree- and plot-level genotype diversity, suggesting that, everything else being equal, dispersal characteristics of the organism may be at least as important as landscape configuration in determining the spatial scale of functional connectivity.

Acknowledgements

References

Antoine M.E. and McCune B. 2004. Contrasting fundamental and realized ecological niches with epiphytic lichen trans-
plants in an old-growth *Pseudotsuga* forest. Bryologist 107: 163–172.

Bailey R. and James P. 1979. Birds and the dispersal of lichen propagules. Lichenologist 11: 105–106.

Bailey R.H. 1976. Ecological aspects of dispersal and establishment in lichens. In: Brown D.H., Hawksworth D.L. and Bailey R.H. (eds), Lichenology: Progress and Problems. Academic Press, London, pp. 215–247.

Beerli P. and Felsenstein J. 1999. Maximum-likelihood estimation of migration rates and effective population numbers in two populations using a coalescent approach. Genetics 152: 763–773.

Brooks C.P. 2003. A scalar analysis of landscape connectivity. Oikos 102: 433–439.

Cain M.L., Milligan B.G. and Strand A.E. 2000. Long-distance seed dispersal in plant populations. Am. J. Bot. 87: 1217–1227.

Clark J.S. 1998. Why trees migrate so fast: confronting theory with dispersal biology and the paleorecord. Am. Nat. 152: 204–224.

Clobert J., Danchin E., Dhondt A.A. and Nichols J.D. (eds) 2001. Dispersal. Oxford University Press, Oxford.

Denison W.C. 2003. Apothecia and ascospores of *Lobaria oregana* and *Lobaria pulmonaria* investigated. Mycologia 95: 513–518.

Fortin M.J., Boots B., Csillag F. and Remmel T.K. 2003. On the role of spatial stochastic models in understanding landscape indices in ecology. Oikos 102: 203–212.

Gardner R.H., Milne B.T., Turner M.G. and O'Neill R.V. 1987. Neutral models for the analysis of broad-scale landscape patterns. Landscape Ecol. 1: 19–28.

Gonzalez-Astorga J.G., Cruz-Angon A., Flores-Palacios A. and Vovides A.P. 2004. Diversity and genetic structure of the Mexican endemic epiphyte *Tillandsia achyrostachys* E. Morr. ex Baker var. *achyrostachys* (Bromeliaceae). Ann. Bot. 94: 545–551.

Goodwin B.J. 2003. Is landscape connectivity a dependent or independent variable? Landscape Ecol. 18: 687–699.

Harrison S. and Bruna E. 1999. Habitat fragmentation and large-scale conservation: what do we know for sure? Ecography 22: 225–232.

Holderegger R., Gugerli F. and Kamm U. in press. Adaptive versus neutral genetic diversity: implications for landscape genetics. Landscape Ecol. 21: 797–807.

Ihaka R. and Gentleman R. 1996. R: a language for data analysis and graphics. J. Comput. Grap. Stat. 5: 299–314.

Jordan W.P. 1970. The internal cephalodia of the genus *Lobaria*. Bryologist 73: 669–681

Kalwij J.M. 2005. Selecting and testing indicators of forest history and sylvopastoral landscape dynamics. Ph.D. Thesis, University of Bern, Bern.

Kalwij J.M., Wagner H.H. and Scheidegger C. (2005). Effects of stand-level disturbance events on the spatial distribution of a lichen indicator of forest conservation value. Ecol. Appl. 15: 2015–2024

Keymer J.E., Marquet P.A., Velasco-Hernandez J.X. and Levin S.A. 2000. Extinction thresholds and metapopulation persistence in dynamic landscapes. Am. Nat. 156: 478–494.

Kot M., Lewis M.A. and vandenDriessche P. 1996. Dispersal data and the spread of invading organisms. Ecology 77: 2027–2042.

Lertzman K. and Fall J. 1998. From forest stands to landscapes: spatial scales and the roles of disturbances. In: Peterson D.L. and Parker V.T. (eds), Ecological Scale: Theory and Applications. Columbia University Press, New York, pp. 339–367.

Merriam G. 1984. Connectivity: a fundamental ecological characteristic of landscape pattern. First International Seminar on Methodology in Landscape Ecological Research and Planning. Roskilde Universitetsforlag GeuRuc, Roskilde.

Ouborg N.J., Piquot Y. and Van Groenendael J.M. 1999. Population genetics, molecular markers and the study of dispersal in plants. J. Ecol. 87: 551–568.

Ozinga W.A., Schaminee J.H.J., Bekker R.M., Bonn S., Poschlod P., Tackenberg O., Bakker J. and van Groenendael J.M. 2005. Predictability of plant species composition from environmental conditions is constrained by dispersal limitation. Oikos 108: 555–561.

Parker M. and Mac Nally R. 2002. Habitat loss and the habitat fragmentation threshold: an experimental evaluation of impacts on richness and total abundances using grassland invertebrates. Biol. Conserv. 105: 217–229.

Peck S.L. 2004. Simulation as experiment: a philosophical reassessment for biological modeling. Trends Ecol. Evol. 19: 530–534.

Ray C. 2001. Maintaining genetic diversity despite local extinctions: effects of population scale. Biol. Conserv. 100: 3–14.

Richards C.M., Church S. and McCauley D.E. 1999. The influence of population size and isolation on gene flow by pollen in *Silene alba*. Evolution 53: 63–73.

Rikkinen J., Oksanen I. and Lohtander K. 2002. Lichen guilds share related cyanobacterial symbionts. Science 297: 357–357.

Rose F. 1976. Lichenological indicators of age and environmental continuity in woodlands. In: Brown H.D., Hawksworth D.L. and Bailey R.H. (eds), Lichenology: Progress and Problems. Academic Press, London, pp. 279–307.

Rose F. 1992. Temperate forest management: its effects on bryophyte and lichen floras and habitats. In: Bates J.W. and Farmer A. (eds), Bryophytes and Lichens in a Changing Environment. Clarendon Press, Oxford, pp. 211–233.

Scheidegger C. 1995. Early development of transplanted isidioid soredia of *Lobaria pulmonaria* in an endangered population. Lichenologist 27: 361–374.

Scheidegger C., Frey B. and Walser J.C. 1998. Reintroduction and augmentation of populations of the endangered *Lobaria pulmonaria*: methods and concepts. In: Kondratyuk S. and Coppins B.J. (eds), Lobarion Lichens as Indicators of the Primeval Forests of the Eastern Carpathians. Kiev, Phytosociocentre, pp. 33–52.

Scheidegger C. and Goward T. 2002. Monitoring lichens for conservation: Red Lists and conservation action plans. In: Nimis P.L., Scheidegger C. and Wolseley P.A. (eds), Monitoring with lichens – monitoring lichens. Kluwer, New York, pp. 163–181.

Schütz J.P. 2002. Silvicultural tools to develop irregular and diverse forest structures. Forestry 75: 329–337.

Snäll T., Pennanen J., Kivisto L. and Hanski I. 2005. Modelling epiphyte metapopulation dynamics in a dynamic forest landscape. Oikos 109: 209–222.

Sork V.L. and Smouse P.E. 2006. Genetic analysis of landscape connectivity in tree populations. Landscape Ecol. 21: 821–836.

Sundberg B., Palmqvist K., Esseen P.A. and Renhorn K.E. 1997. Growth and vitality of epiphytic lichens. 2. Modelling of carbon gain using field and laboratory data. Oecologia 109: 10–18.

Tackenberg O. 2003. Modeling long-distance dispersal of plant diaspores by wind. Ecol. Monogr. 73: 173–189.

Taylor P.D., Fahrig L., Henein K. and Merriam G. 1993. Connectivity is a vital element of landscape structure. Oikos 68: 571–573.

Tischendorf L. and Fahrig L. 2000. How should we measure landscape connectivity? Landscape Ecol. 15: 633–641.

Trapnell D.W. and Hamrick J.L. 2005. Mating patterns and gene flow in the neotropical epiphytic orchid, *Laelia rubescens*. Mol. Ecol. 14: 75–84.

Villa F., Voinov A., Fitz C. and Costanza R. 2004. Calibration of large spatial models: a multistage, multiobjective optimization technique. In: Costanza R. and Voinov A. (eds), Landscape Simulation Modeling: A Spatially Explicit, Dynamic Approach. Springer, New York, pp. 77–116.

Vittoz P. 1998. Flore et végétation du Parc jurassien vaudois: typologie, écologie et dynamiqu des milieux. Ph.D. Thesis, Université de Lausanne, Lausanne.

Wagner H.H. and Fortin M.J. 2005. Spatial analysis of landscapes: concepts and statistics. Ecology 86: 1975–1987.

Wagner H.H., Holderegger R., Werth S., Gugerli F., Hoebee S.E. and Scheidegger C. 2005. Variogram analysis of the spatial genetic structure of continuous populations using multilocus microsatellite data. Genetics 169: 1739–1752.

Walser J.C. 2004. Molecular evidence for limited dispersal of vegetative propagules in the epiphytic lichen *Lobaria pulmonaria*. Am. J. Bot. 91: 1273–1276.

Walser J.C., Gugerli F., Holderegger R., Kuonen D. and Scheidegger C. 2004. Recombination and clonal propagation in different populations of the lichen *Lobaria pulmonaria*. Heredity 93: 322–329.

Walser J.C., Sperisen C., Soliva M. and Scheidegger C. 2003. Fungus-specific microsatellite primers of lichens: application for the assessment of genetic variation on different spatial scales in *Lobaria pulmonaria*. Fungal Genet. Biol. 40: 72–82.

Walser J.C., Zoller S., Buchler U. and Scheidegger C. 2001. Species-specific detection of *Lobaria pulmonaria* (lichenized ascomycete) diaspores in litter samples trapped in snow cover. Mol. Ecol. 10: 2129–2138.

Werth S. 2005. Dispersal and persistence of an epiphytic lichen in a dynamic pasture-woodland landscape. Ph.D. Thesis, University of Bern, Bern.

Werth S., Wagner H.H., Holderegger R., Kalwij J.M. and Scheidegger C. in press. Effect of disturbances on the genetic diversity of an old-forest associated lichen. Mol. Ecol.

Wiens J.A., Stenseth N.C., Van Horne B. and Ims R.A. 1993. Ecological mechanisms and landscape ecology. Oikos 66: 369–380.

With K.A. 1997. The application of neutral landscape models in conservation biology. Conserv. Biol. 11: 1069–1080.

With K.A., Cadaret S.J. and Davis C. 1999. Movement responses to patch structure in experimental fractal landscapes. Ecology 80: 1340–1353.

Yoshimura I. 1971. The genus *Lobaria* of Eastern Asia. J. Hattori Bot. Lab. 34: 231–364.